Wearable 3D Shape Display for Dynamic Interfaces Rendering

Bilige Yang[1,2], Benjamin Stephens-Fripp[1], Priyanshu Agarwal[1], Sonny Chan[1], Nathan Usevitch[1], Andrew Stanley[1], and Yatian Qu[1,*]

2023 IEEE World Haptics Conference (WHC) | 979-8-3503-9993-6/23/$31.00 ©2023 IEEE | DOI: 10.1109/WHC56415.2023.10224493

***Abstract*— Recreating the feeling of touch is crucial for seamless interactions with objects in the virtual world. Many haptic solutions exist in the forms of graspable, wearable, and touchable systems for recreating kinesthetic and tactile feedback. Yet, to the best of our knowledge, no wearable system to date can directly render dynamic shapes in user's hand with drastic shape rendering capabilities. We present a wearable 3D haptic display with drastic shape change and dynamic signal rendering. We explored direct physical and dynamic rendering of shapes in users' hands using a 3D lattice of pneumatic actuators– a direct-embodiment approach. We also conducted user studies to determine the efficacy of the shape and frequency rendering and found the results to be generally convincing.**

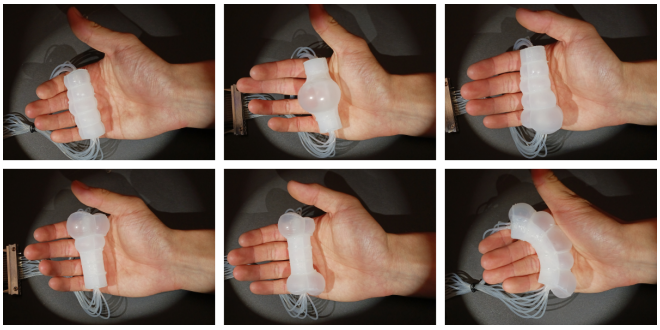

Fig. 1. Wearable 3D shape display for dynamic interfaces rendering. Some shapes generated by the device.

I. INTRODUCTION

The sense of touch is crucial for realistic interactions in virtual and augmented realities (VR/AR) [1], [2]. Many virtual environments allow interactions with the virtual objects. Yet, despite the wide range of shapes, sizes, and textures of the objects present in the virtual world, interaction with the human hands comes, in most cases, in the form of a rigid, fixed-shape controller. There have been promising recent efforts in bringing advances in haptics to the field of VR/AR. We provide a brief overview below to expound the advantages and disadvantages of these efforts and how our work fills an important gap in the haptics literature for applications in VR/AR.

Efforts in haptics can be generally divided into three categories based on the method of interaction and form factors: graspable, wearable, and touchable systems [3]. Graspable devices are usually kinesthetic (force-feedback) devices that are grounded or ungrounded, that allow the user to push on them (and be pushed back) [4], [5], [6], [7], [8], [9], [10]. Wearable systems are typically tactile (cutaneous) devices that are mounted to the hands or other parts of the body and display sensations such as vibration, lateral skin stretch, and normal skin deformation [11], [12], [13], [14]. Touchable systems are encountered-type displays that allow the user to actively explore the entire surface [15], [16], [17], [18], [19].

To reconstruct shapes in the virtual environment, all three categories can be employed for different effects. Graspable devices provide accurate positional and force feedback. Yet graspable systems seem to have challenges to render a large variety of shapes, with the rendering usually limited to just one or two dimensions of linear force scales. In addition, graspable devices are mostly capable of rendering rigid objects. Rendering of soft or deformable objects is a currently a gap. Wearable systems provide great mobility and versatility with regard to object location and size. Yet wearable systems do not provide good force response and the amount of normal forces simulated is typically small. Touchable systems allow for more user exploration and a more holistic, realistic experience. Yet most touchable systems are limited to 2D or 2.5D in dimensions with one movable axis. Recently, there has been work on developing a soft 3D haptic shape display [20]. However, all of the reported display systems are mostly bulky, cumbersome and stationary.

Our goal is to develop a device that is able to directly embody shapes but stay wearable in user's hand, so that users can freely explore the shapes and eliminate the many problems with sensing and actuation that are present in the graspable and wearable systems. In addition, we would like to explore the potential of rendering both rigid and soft objects. Such shape changing controllers have been explored to a limited extent, as outlined below.

Researchers used mobile platform with pin array on a small hand-held device to display some shapes, but the shape rendering is limited to 2D with small displacement and rigid pins [15], [21]. Kovacs et al. created a binary shape device with a ball that can swing into or out of the user's hand [22], which can be useful for some interesting use cases (like an apple picking game), but not generally applicable to more interactive scenarios. We need a shape-rendering device that has more granularity than binary on/off.

There have also been works where the weight distribution on the controller can be changed to generate variable moment of inertia to create illusions of holding different objects [23], [24]. Yet, here the actual shape in the user's hand does

[1]Meta Reality Labs, Redmond, WA 98052, USA
[2]Department of Mechanical Engineering and Materials Science, Yale University, CT 06511, USA
* Corresponding Author

not change and the amount of shape variation is limited. There has been shape changing controller with one moveable extruded part that pops up to simulate the reactive force in the virtual environment [25], but the shape generated is simple and one dimensional, not realistic enough for a wider range of other common objects and shapes.

Inflatable pouches have been integrated with VR to show common shapes like cylinders and spheres [26], [27], but the pouches are non-stretchable and thus fixed in their final shape without the ability to render smaller or bigger shapes, as well as any curvature. Shape and texture rendering have been experimented with on a revolving touch device that presents shape and texture based on virtual environment cues [28]. But the shape interaction is limited to one finger tip and the range of shapes generated is limited to the shapes present on the revolver.

The most relevant existing work to ours is a handheld device with mechanical gearing and movable tiles to render shapes with different circumferences [29]. This device can render a wider range of objects than the previous mentioned devices but the shape change is still subtle due to the small and symmetric displacement generated by the tile mechanism.

In this study, we are presenting a wearable 3D display with drastic shape change, where the device showed more than 50% volume change than the original body (see Fig. 1). Our device demonstrated the rendering of a range of primitive shapes and the ability to incorporate frequency signals. To our knowledge, our works is the first work that actively exploits the combination of frequency and shape signals for haptic rendering.

Specifically, we make the following contributions in this work:

- We introduced a 5-stack 3D pneumatic lattice actuator with 15 individually addressable chambers, which is capable of rendering a wide range of static shapes as well as dynamic frequencies.
- We showed our device to be over 90% accurate in rendering static shapes and over 80% accurate in rendering distinguishable frequency signals in user studies.
- We demonstrated that multi-modal (shape and frequency) inputs generated higher distinguishability in haptic user studies.
- We introduced touch sensing based solely on pneumatics for the actuator to close the feedback loop.
- Although with limited demonstration in this work, we believe our device has the potential to render both rigid and soft objects with additional features, such as adding strain-limiting mechanism.

The rest of the paper is divided into the following sections: Device and Methods, User Studies, and Results and Discussions.

II. Device and Methods

Our haptic device consists of five molded silicone stacks. Each stack includes three individually controlled chambers. The device is shown in Fig. 1. In the following sections, we will describe in detail how we fabricated our device and the supporting hardware and software architecture used for shape rendering.

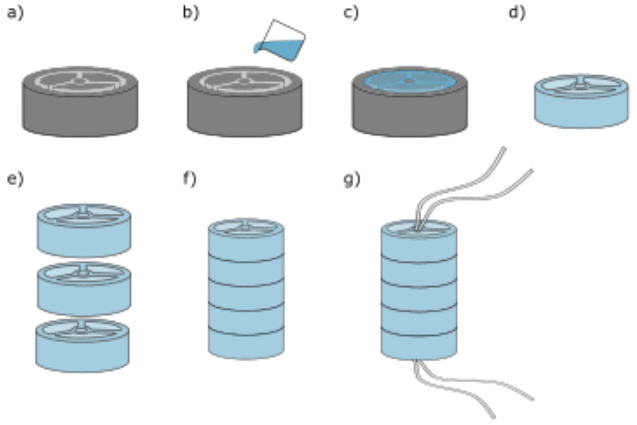

Fig. 2. Fabrication of the actuator. a) 3D print the mold with three-chamber design. b) Pour in uncured silicone. c) Let silicone cure. d) Demold for one stack of the silicone actuator (with three chambers). e) Repeat the above steps for multiple stacks. f) Bond stacks vertically with silicone adhesive. g) Attach tubing into each of the chambers with silicone adhesive.

A. Actuator Fabrication

We fabricated the actuators by molding silicone using 3D printed molds, as illustrated in Figure 2. First, we printed the molds using a Form 2 stereo-lithography (SLA) 3D printer (Formlabs, USA), with a slightly deformable resin for easier demolding (Tough 1500 Resin, Formlabs, USA). Uncured silicone mixture made with DragonSkin 10 part A and B (Smooth-On, USA) was poured into the mold and cured at 80 $^{\circ}C$ for 2 hours. This is for one layer (or stack) of the final actuator. Note that due to the three cavities created by the mold, each stack has three individually addressable chambers. Five layers are fabricated using the exact same process. After individual layers of the actuator were created, all five layers, together with a bottom sealing layer were glued onto each other with more uncured DragonSkin 10 silicone. After the whole body of the silicone actuator was made, silicone tubings were connected to each of the 15 individual chambers (3 chambers $\times$ 5 stacks) and glued in place with Silpoxy silicone glue (Smooth-On, USA). Our manufacturing process of the device is simple, straightforward and low-cost. We could potential extend the device to a larger number of stacks if needed.

B. Electronics and Control

We control each pneumatic chamber (out of the 15 total) through a pressure regulator (Festo VEAB, 1-200 kPa) individually (Fig. 3). The 15 pressure regulators were controlled using an analog output generated through a data acquisition device (NI cDAQ-9174 with NI9264 module) interfaced with a PC. For more information on the pneumatic and electronic control hardware, please see more details in the previously published work [30].

TABLE I
ACTUATOR PHYSICAL DETAILS

Property	Value
Dimensions	6.5cm x 2.3cm x 2.3cm
Weight	18.5g
Minimum Diameter	2.30cm
Maximum Diameter	7.32cm
Maximum Pressure	7.7psi
Rendering time (Maximum Inflation)	5.2 seconds

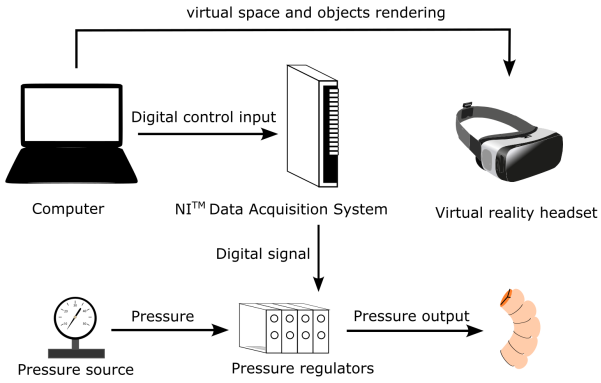

Fig. 3. Electronics and control hardware setup for the actuator.

C. Software Integration

We used MATLAB (MathWorks, USA) on the PC to interface with the aforementioned data acquisition device and pressure regulators. We also created a virtual reality environment using Unreal Engine 4 (Epic Games, USA) for the user study, to be described below. Hand tracking on the Oculus Quest 2 headset was enabled using the Oculus API.

D. Shape Rendering

Shape rendering via direct embodiment is based on the realization that 3D shapes are simply volumes that are occupied by an object in 3D space. Thus, if a device can fill the exact (or approximate) volume that would have been filled by certain shapes, the device renders that shape for the user. The accuracy for shape rendering with the direct embodiment approach relies on the granularity of the actuator that fills such a space.

Our pneumatic actuator has 15 individually addressable chambers as a 3D lattice that can inflate to fill volumes to approximate shapes in 3D space. The overall system operation principle is as follows: The MATLAB software controls the 15 pressure regulators to hold at specific pressures, respectively. As a result, the 15 chambers in the actuators are actuated to different sizes that geometrically combine to become the final shape in the user's hand. For example, to achieve the simple cylinder shape, we inflated all 15 chambers in the actuator at a fixed low pressure (5 psi, in one case). And for a curved shape like a banana, only 5 chambers on one side of the actuator were inflated, causing the actuator to bend into a curve. The procedure applies for various shapes in static shape rendering.

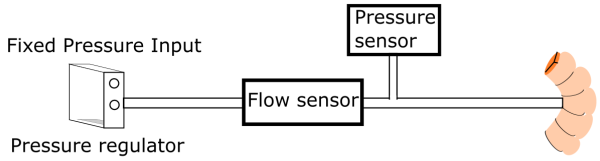

Fig. 4. Touch sensing hardware setup.

To give user the feeling of frequency or vibrations, the pressure regulator can output a sinusoidal pressure wave around a fixed pressure baseline. This pressure baseline determines the static shape being rendered on the actuator while the sinusoidal pressure wave gives the feeling of vibration at different frequencies.

We note that although the device was connected to the pneumatic control system through silicone tubing, the tubing volume is a small fraction of the total volume of the device. Therefore, squeezing the device will not push significant amount of air into the tubing. In addition, our pneumatic control system (as described in Section II.B) uses 3-way valves to control the air flow. As a result, we do not anticipate that different grasping forces would influence the shape rendering and perception in our user studies.

E. Touch Sensing via Pressure and Flow Sensors

To provide feedback on the instance of contact with our actuator, we needed to have touch sensing on the actuator, so that if the actuator is grasped by the user, the computer program can register such an event. We experimented with a touch sensing setup on our actuator, simply using a flow sensor (Honeywell Zephyr Series Digital Airflow Sensors HAFUHT0010L4AXT) and a pressure sensor (Honeywell 26PCDFG5G39), as shown in Fig. 4. The pressure sensor registers the instantaneous pressure inside one of the actuator chambers. The flow sensor registers the mass flow in the pneumatic tubing that is connected to the actuator chamber, with the positive flow direction being air going into the actuator.

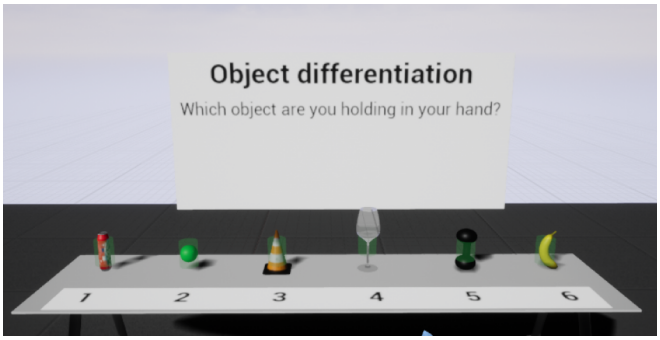

Fig. 5. User study one: static object discrimination. What the user sees in the headset.

III. User Studies

To fully show the capability of our device, we conducted user studies for both static object discrimination (study one) and dynamic object discrimination (study two). We recruited 22 users in total (11 males and 11 females), between the age 23 and 56. Users were all right-handed. For both study one and study two, the user wears a virtual reality headset (Oculus Quest 2, Meta Platforms, USA) while holding the actuator in their dominant (right) hand.

A. Static Object Discrimination Study

For study one, the user needs to distinguish between 6 rendered objects (coke can, tennis ball, cone, wine glass, dumbbell, and banana). In the headset, the user sees the six target objects placed on a table in front of them (see Fig. 5). The user also sees the prompt "Which object are you holding in your hand?" The actuator in user's hand will actuate and render one out of the six shapes on the table. The user will then tell the test giver which shape the user thinks is the shape being rendered. There were 18 trials (6 objects each appearing 3 times randomly) for each user. Their responses were recorded.

B. Dynamic Object Discrimination Study

For study two, the user needs to distinguish 3 dynamic scenarios: a beating heart, a flopping fish, and a vibrating motorcycle handle (Fig. 6). These three scenarios each have their distinct shapes as well as dynamic frequencies, as shown in Fig. 7. The beating heart has a round shape with a frequency of 1Hz (1 beat per second). The flopping fish has a curved shape with a frequency of 3Hz (3 flaps per second). The motorcycle handle has a cylindrical shape with a frequency of 6Hz (6 vibrations per second).

The user experienced these 3 scenarios under three different stages, as described below. We note that users were not provided any prior training or given feedback after each stage of the user studies. Therefore, we think the following scenarios represent the reasonable accuracy of shape rendering results for each stage.

I. In the first stage, the user was given both the shape information and the frequency information for the scenarios. For example, the beating heart would render as a round shape with 1Hz beating frequency. The user was instructed to make guesses as to which scenario was rendered for 9 trials (each scenario appeared 3 times randomly).

II. In the second stage, the user was only given the shape information, without frequency information. For example, the beating heart rendered as a round shape, but without the beating frequency. The user was instructed to make guesses as to which scenario was rendered for 9 trials (each scenario appeared 3 times randomly).

III. In the third stage, the shapes were kept the same as a cylinder for all the scenarios and the user was only given the frequency cues. For example, the beating heart was rendered as a cylinder with a vibration at frequency of 1Hz. The user was instructed to make guesses as to which scenario was rendered for 9 trials (each scenario appeared 3 times randomly). Their responses were recorded.

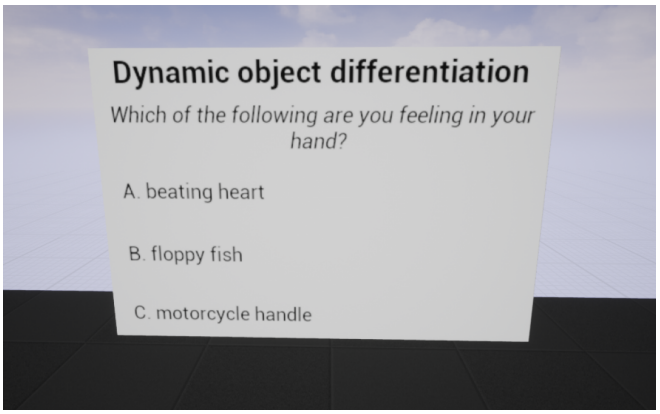

Fig. 6. User study two: dynamic object discrimination test. What the user sees in the headset.

IV. Results and Discussions

A. Shape Rendering Actuator

The fabricated full 5-stack 15-chamber actuator has a dimension of 6.5cm x 2.3cm x 2.3cm, about the size of a thick whiteboard marker when not actuated. This size fits well in most people's hand and not obstructive when the user's fingers move around in motions other than grasping. More physical details about the actuator are shown in Table 1. We note that in the current version of the device, we asked the users to hold the device in user studies. However, it is straightforward to attach an adjustable strap to the 5-stack actuator device to make it wearable.

The actuator can actuate to its maximum inflated shape (about 300% of original diameter) in about 5.2 seconds under a maximum pressure of 7.7 psi. The actuator's inflated can be accurately controlled with pressure input due to the direct correlation between pressure and shape circumference in the actuator (See Fig. 8). The large amount of shape change (300%) enabled by this actuator allows for a wide range of objects being rendered. The speed of the shape change (5.2 seconds to max inflation) also enables adaptive behaviors in virtual environment, such as changing of objects grabbed and

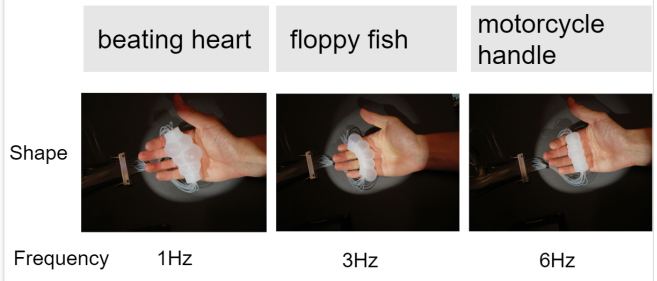

Fig. 7. User study two: three scenarios generated by the actuator (with shape and frequency information).

dynamic shape changes. The shape changing speed and the range of vibration frequencies are functions of the input pressure, actuator stack volume and actuator materials. Future devices can be optimized for specific rendering applications.

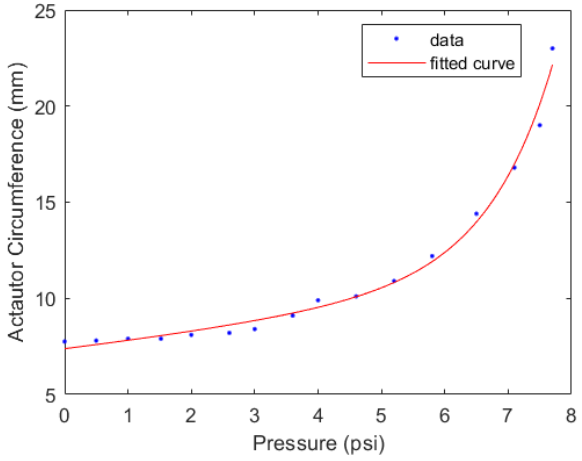

Fig. 8. Plot of actuator circumference in one stack as a function of pressure in the chamber, with all three segments within the stack being pressurized.

B. Touch Sensing via Pressure and Flow Sensors

The results shown in Fig. 9 indicated that a pressure sensor and a flow sensor can both provide high-quality distinguishable signal in the event of actuator being touched. Specially, with a baseline inflation pressure at 4 psi, the pressure sensor registered a 10% pressure increase with the onset of squeezing the actuator. And the flow sensor registered about 0.25 SLPM with the onset of squeezing the actuator. This experiment demonstrates a possible implementation of touching sensing method with our actuator that is purely pneumatic, with no additional sensors needed on the actuator itself.

This touch sensing mechanism greatly simplifies the architecture on the side of the actuator and can scale with the number of chambers in the actuators without added complexities.

C. Static Object Discrimination Study

In user study one, we investigated what is the accuracy of static shape rendering in user's hand. From the images of the rendered shapes (Fig. 10), we can see the actuated shapes and the shapes that the actuator attempted to mimic.

The confusion matrix in Fig. 11 shows quantitative results of whether the user was able to distinguish the shapes formed by the actuator in their hand. Overall, the accuracy is 90.7% for all six shapes combined. Individually, we see that the coke can (shape No.1) was the least recognizable shape with identification accuracy of 83.3%, likely due to the lack of features. And the tennis ball (shape No.2) was the most recognizable shape with accuracy of 95.5%, likely due to its uniquely large volumetric differential between different chambers. The two most confused shapes were coke can and wine glass– this might be a result of confusion on the

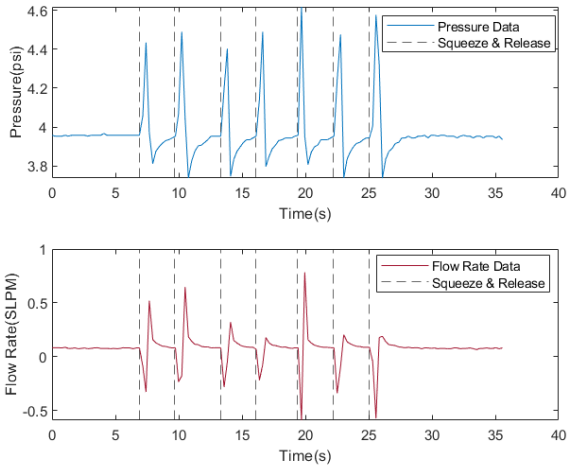

Fig. 9. Data plot for touch sensing via pressure and flow sensors.

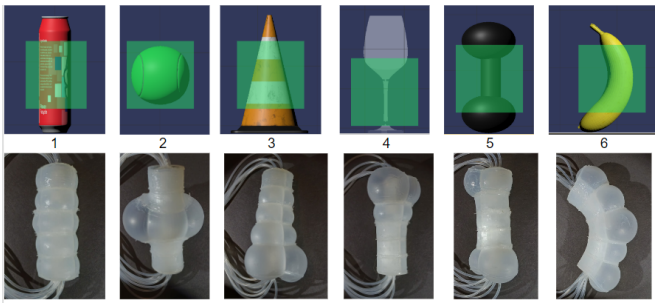

Fig. 10. User study one: six shapes that the user sees in VR compared to the shapes generated by the actuator.

location of grasping since the stem of the wine glass is also a nicely shaped cylinder.

Overall, the first user study has shown that users can distinguish well (with over 90% accuracy) of the static shapes generated by our actuator. This provides the basis that our direct embodiment approach works well for static shapes.

D. Dynamic Object Discrimination Study

In user study two, we first tested how accurate users can identify three haptic scenarios (a beating heart, a flopping fish, and a vibrating motorcycle handle) with both shape and frequency information (Fig. 12). We observed that with both shape and frequency signals, the users can identify the scenarios with an accuracy of 96%. When the users have only frequency signals, the overall identification accuracy dropped to 83.5%. When the user have only shape signals, the overall identification accuracy was 88.6%, also lower than the case with both shape and frequency signals. Clearly, when users have access to more streams of signals for a given scenario, the users were more likely to guess the right shapes.

In the frequency signal-only stage, users mostly confused the flopping fish and the motorcycle handle (Fig. 13). This confusion is likely due to that the vibration frequencies for floppy fish and vibrating motorcycle handle are only

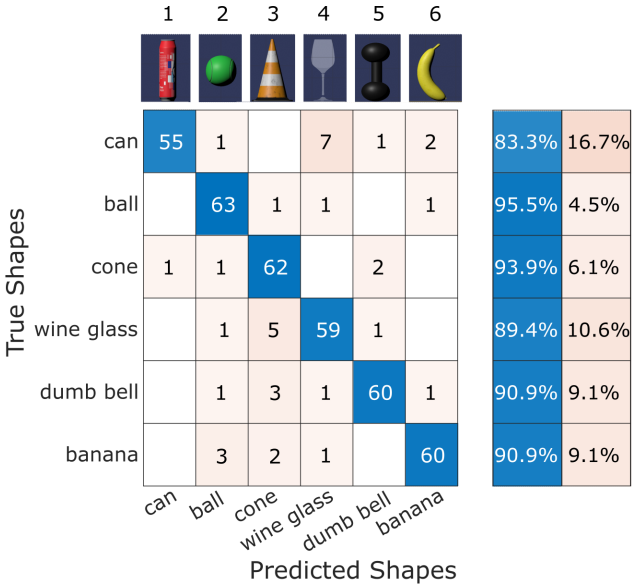

Fig. 11. User study one result: confusion matrix for the six shapes generated by the actuator. The number in the matrix indicates the number of guesses. Blue color shows correct guesses where pink color shows incorrect guesses. The column on the right is the cumulative percentage of correct and incorrect guesses for each shape.

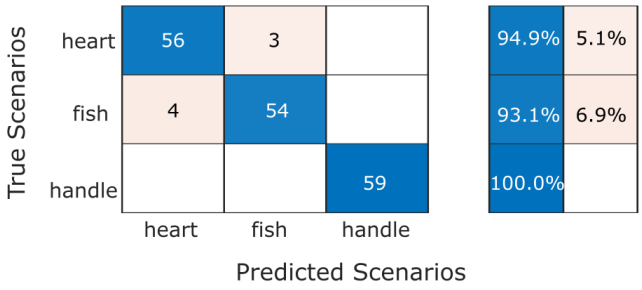

Fig. 12. User study two result: confusion matrix for the three scenarios with both shape and frequency cues. The number in the matrix indicates the number of guesses. Blue color shows correct guesses where pink color shows incorrect guesses. The column on the right is the cumulative percentage of correct and incorrect guesses for each scenario.

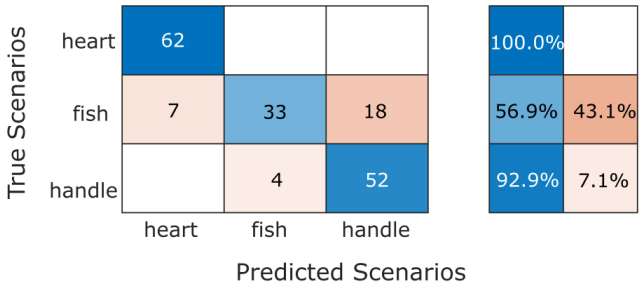

Fig. 13. User study two result: confusion matrix for the three scenarios with only frequency cues. The number in the matrix indicates the number of guesses. Blue color shows correct guesses where pink color shows incorrect guesses. The column on the right is the cumulative percentage of correct and incorrect guesses for each scenario.

2X different (3 Hz vs. 6 Hz) and the 3 Hz difference in frequencies can be difficult to discern without the help of shape information. We anticipated that higher frequencies for vibrating motorcycle might help reduce the confusion. Our device can be optimized for future iterations to enable high-frequency rendering.

In the shape signal-only stage, users mostly confused the heart and the motorcycle handle (Fig. 14). This confusion can be explained by noting both the heart and the handle have a positive curvature on them, unlike the fish with a negative curve. So the heart and the handle were more easily confused with the frequency information.

There are two noteworthy details. First is that the shape only signals made the users have an accuracy of 88.6%, which is close to the accuracy shown in shape identification task (90.7%) in User Study One. The shape-only result could serves as another experimental data set of shape rendering accuracy, further confirming the results in the static shape study.

The second noteworthy detail is that the frequency-only and shape-only tests were run on the same participants who were first tested with shape-and-frequency-together conditions. The participants already had experienced the shape and frequency signals so that the tests later should have a higher accuracy due to familiarity. This detail strengthens our result, since with the learning, the users still did worse with single signal streams than dual signal streams.

Overall, the user study here has shown that the actuator can render dynamic signals well for the users. The study has also shown that dual inputs (shape and frequency) for the haptic scenario allow for higher accuracy in dynamic discrimination studies.

V. Conclusions

The 5-stack 15-chamber actuator was successful in rendering primitive grasping shapes (cylinder, sphere, and hook), as well as more complicated curvatures like a dumbbell and cone. We can forecast that pneumatically-driven, volumetrically expanding soft actuators can provide increasingly better shape rendering with an increasing number of individually addressable actuators. The actuators could also render dynamic shapes with frequency information. This has not been shown extensively before. We have shown that with multiple streams of information (shape and frequency), the user can recognize scenarios easier. Overall, we have demonstrated a shape rendering device that is light, wearable, and able to change into various shapes and curvatures with frequency rendering. We believe this opens up new avenues in haptics research for more versatile handheld devices that are capable of realistic haptic feedback.

In summary, our work demonstrated:

1) A 5-stack, 15-chamber pneumatic 3D lattice actuator that is capable of rendering static and dynamic shape.
2) Touch sensing on the pneumatic actuator with only a pressure sensor and a flow sensor.

We performed users studies: static object discrimination study and dynamic object discrimination study. Our key findings from the user studies were:

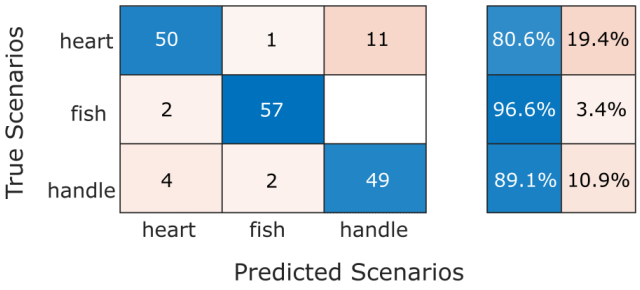

Fig. 14. User study two result: confusion matrix for the three scenarios with only shape cues. The number in the matrix indicates the number of guesses. Blue color shows correct guesses where pink color shows incorrect guesses. The column on the right is the cumulative percentage of correct and incorrect guesses for each scenario.

1) Users identified objects with over 90% accuracy for six shapes in the static shape rendering tests.
2) Users identified objects with over 80% accuracy for three scenarios in the dynamic shape rendering tests.
3) Multi-modal (shape and frequency) inputs generated higher distinguishability in haptic user studies.

Some areas for future work include:

1) Increasing the number of chambers in the actuator for higher resolution of rendering.
2) Fully incorporating the touch sensing into the software pipeline for a virtual reality shape rendering demonstration.
3) Investigating the role of stiffness (as a result of inflation) in user's perception of object rendering. Potentially adding stiffness rendering capability through methods such as strain-limiting.

ACKNOWLEDGMENT

B.Y. would like to thank Wenyang Pan, Brendon Beardsley, Robert Hunt, and Tharm Sribhibhadh for help with fabrication and equipment operations.

ACKNOWLEDGMENT

REFERENCES

[1] W. Dangxiao, G. Yuan, L. Shiyi, Y. Zhang, X. Weiliang, and X. Jing, "Haptic display for virtual reality: progress and challenges," *Virtual Reality & Intelligent Hardware*, vol. 1, no. 2, pp. 136–162, 2019.
[2] C. Bermejo and P. Hui, "A survey on haptic technologies for mobile augmented reality," *ACM Computing Surveys (CSUR)*, vol. 54, no. 9, pp. 1–35, 2021.
[3] H. Culbertson, S. B. Schorr, and A. M. Okamura, "Haptics: The present and future of artificial touch sensation," *Annual Review of Control, Robotics, and Autonomous Systems*, vol. 1, no. 1, pp. 385–409, 2018.
[4] "Dexta robotics." [Online]. Available: https://origin.dextarobotics.com/
[5] J. Blake and H. B. Gurocak, "Haptic glove with mr brakes for virtual reality," *IEEE/ASME Transactions On Mechatronics*, vol. 14, no. 5, pp. 606–615, 2009.
[6] M. Bouzit, G. Burdea, G. Popescu, and R. Boian, "The rutgers master ii-new design force-feedback glove," *IEEE/ASME Transactions on mechatronics*, vol. 7, no. 2, pp. 256–263, 2002.
[7] I. Choi, H. Culbertson, M. R. Miller, A. Olwal, and S. Follmer, "Grabity: A wearable haptic interface for simulating weight and grasping in virtual reality," in *Proceedings of the 30th Annual ACM Symposium on User Interface Software and Technology*, 2017, pp. 119–130.
[8] C. Fang, Y. Zhang, M. Dworman, and C. Harrison, "Wireality: Enabling complex tangible geometries in virtual reality with worn multi-string haptics," in *Proceedings of the 2020 CHI Conference on Human Factors in Computing Systems*, 2020, pp. 1–10.
[9] H. In, K.-J. Cho, K. Kim, and B. Lee, "Jointless structure and under-actuation mechanism for compact hand exoskeleton," in *2011 IEEE International Conference on Rehabilitation Robotics*. IEEE, 2011, pp. 1–6.
[10] I. Choi, E. W. Hawkes, D. L. Christensen, C. J. Ploch, and S. Follmer, "Wolverine: A wearable haptic interface for grasping in virtual reality," in *2016 IEEE/RSJ International Conference on Intelligent Robots and Systems (IROS)*. IEEE, 2016, pp. 986–993.
[11] H. Benko, C. Holz, M. Sinclair, and E. Ofek, "Normaltouch and texturetouch: High-fidelity 3d haptic shape rendering on handheld virtual reality controllers," in *Proceedings of the 29th annual symposium on user interface software and technology*, 2016, pp. 717–728.
[12] J. Lee, M. Sinclair, M. Gonzalez-Franco, E. Ofek, and C. Holz, "Torc: A virtual reality controller for in-hand high-dexterity finger interaction," in *Proceedings of the 2019 CHI conference on human factors in computing systems*, 2019, pp. 1–13.
[13] T. M. Simon, R. T. Smith, and B. H. Thomas, "Wearable jamming mitten for virtual environment haptics," in *Proceedings of the 2014 ACM International Symposium on Wearable Computers*, 2014, pp. 67–70.
[14] R. Hinchet, V. Vechev, H. Shea, and O. Hilliges, "Dextres: Wearable haptic feedback for grasping in vr via a thin form-factor electrostatic brake," in *Proceedings of the 31st Annual ACM Symposium on User Interface Software and Technology*, 2018, pp. 901–912.
[15] C. Harrison and S. E. Hudson, "Providing dynamically changeable physical buttons on a visual display," in *Proceedings of the SIGCHI Conference on Human Factors in Computing Systems*, 2009, pp. 299–308.
[16] D. Leithinger, S. Follmer, A. Olwal, and H. Ishii, "Shape displays: Spatial interaction with dynamic physical form," *IEEE computer graphics and applications*, vol. 35, no. 5, pp. 5–11, 2015.
[17] A. F. Siu, E. J. Gonzalez, S. Yuan, J. B. Ginsberg, and S. Follmer, "Shapeshift: 2d spatial manipulation and self-actuation of tabletop shape displays for tangible and haptic interaction," in *Proceedings of the 2018 CHI Conference on Human Factors in Computing Systems*, 2018, pp. 1–13.
[18] L. Yao, R. Niiyama, J. Ou, S. Follmer, C. Della Silva, and H. Ishii, "Pneui: pneumatically actuated soft composite materials for shape changing interfaces," in *Proceedings of the 26th annual ACM symposium on User interface software and Technology*, 2013, pp. 13–22.
[19] A. A. Stanley, J. C. Gwilliam, and A. M. Okamura, "Haptic jamming: A deformable geometry, variable stiffness tactile display using pneumatics and particle jamming," in *2013 World Haptics Conference (WHC)*. IEEE, 2013, pp. 25–30.
[20] M. Koehler, N. S. Usevitch, and A. M. Okamura, "Model-based design of a soft 3-d haptic shape display," *IEEE Transactions on Robotics*, vol. 36, no. 3, pp. 613–628, 2020.
[21] S. Yoshida, Y. Sun, and H. Kuzuoka, "Pocopo: Handheld pin-based shape display for haptic rendering in virtual reality," in *Proceedings of the 2020 CHI Conference on Human Factors in Computing Systems*, 2020, pp. 1–13.
[22] R. Kovacs, E. Ofek, M. Gonzalez Franco, A. F. Siu, S. Marwecki, C. Holz, and M. Sinclair, "Haptic pivot: On-demand handhelds in vr," in *Proceedings of the 33rd Annual ACM Symposium on User Interface Software and Technology*, 2020, pp. 1046–1059.
[23] J. Shigeyama, T. Hashimoto, S. Yoshida, T. Aoki, T. Narumi, T. Tanikawa, and M. Hirose, "Transcalibur: weight moving vr controller for dynamic rendering of 2d shape using haptic shape illusion," in *ACM SIGGRAPH 2018 Emerging Technologies*, 2018, pp. 1–2.
[24] A. Zenner and A. Krüger, "Shifty: A weight-shifting dynamic passive haptic proxy to enhance object perception in virtual reality," *IEEE transactions on visualization and computer graphics*, vol. 23, no. 4, pp. 1285–1294, 2017.
[25] Y. Sun, S. Yoshida, T. Narumi, and M. Hirose, "Pacapa: A handheld vr device for rendering size, shape, and stiffness of virtual objects in tool-based interactions," in *Proceedings of the 2019 CHI conference on human factors in computing systems*, 2019, pp. 1–12.
[26] S.-Y. Teng, T.-S. Kuo, C. Wang, C.-h. Chiang, D.-Y. Huang, L. Chan, and B.-Y. Chen, "Pupop: Pop-up prop on palm for virtual reality," in *Proceedings of the 31st Annual ACM Symposium on User Interface Software and Technology*, 2018, pp. 5–17.

[27] S.-P. Hu and J.-H. Hou, "Pneu-multi-tools: Auto-folding and multi-shapes interface by pneumatics in virtual reality," in *Adjunct Proceedings of the 32nd Annual ACM Symposium on User Interface Software and Technology*, 2019, pp. 36–38.

[28] E. Whitmire, H. Benko, C. Holz, E. Ofek, and M. Sinclair, "Haptic revolver: Touch, shear, texture, and shape rendering on a reconfigurable virtual reality controller," in *Proceedings of the 2018 CHI conference on human factors in computing systems*, 2018, pp. 1–12.

[29] E. J. Gonzalez, E. Ofek, M. Gonzalez-Franco, and M. Sinclair, "X-rings: A hand-mounted 360 shape display for grasping in virtual reality," in *The 34th Annual ACM Symposium on User Interface Software and Technology*, 2021, pp. 732–742.

[30] B. Stephens-Fripp, A. Israr, and C. Rognon, "A multichannel pneumatic analog control system for haptic displays: Multichannel pneumatic analog control system (mpacs)," in *Extended Abstracts of the 2021 CHI Conference on Human Factors in Computing Systems*, 2021, pp. 1–7.